Research Square

Preprints are preliminary reports that have not undergone peer review.
They should not be considered conclusive, used to inform clinical practice,
or referenced by the media as validated information.

Feasibility-Screened SINR Matching and Actual-Power CCP for Sum-Rate Maximization in Downlink PD-NOMA Networks

Murad Halabouni
Multimedia University
Mardeni Bin Roslee
mardeni.roslee@mmu.edu.my

Multimedia University
Sufian Mousa Mitani
Next Generation Network Research Institute, Telekom Malaysia Research & Development
Azwan Bin Mahmud
Multimedia University

Research Article

Keywords: Power-domain NOMA, SINR-based matching, resource allocation, DC programming, convex-concave procedure, sum-rate maximization

Posted Date: November 13th, 2026

DOI: https://doi.org/10.21203/rs.3.rs-11354501/v1

License: This work is licensed under a Creative Commons Attribution 4.0 International License.
Read Full License

Additional Declarations: No competing interests reported.

Feasibility-Screened SINR Matching and Actual-Power CCP for Sum-Rate Maximization in Downlink PD-NOMA Networks

Murad Halabouni [1], Mardeni Bin Roslee [1], Sufian Mousa Mitani [2], Azwan Bin Mahmud [3]

[1] Centre for Wireless Technology, Faculty of Artificial Intelligence and Engineering, Multimedia University, Cyberjaya, 63100, Malaysia
[2] Next Generation Network Research Institute, Telekom Malaysia Research & Development, Cyberjaya 63000, Malaysia
[3] Faculty of Artificial Intelligence and Engineering, Multimedia University Cyberjaya 63000, Malaysia

Corresponding Author:
Mardeni Bin Roslee [1]
Multimedia University, Cyberjaya Campus: 63100 Cyberjaya, Malaysia
Email address: mardeni.roslee@mmu.edu.my

Abstract— The throughput advantage of power-domain non-orthogonal multiple access (PD-NOMA) depends on two coupled decisions: selecting decodable user pairs and allocating powers without violating quality-of-service (QoS), successive-interference-cancellation (SIC), ordering, and total-power constraints. This paper proposes a two-stage framework that first constructs feasibility-screened signal-to-interference-plus-noise ratio (SINR) preferences and then optimizes the actual strong- and weak-user powers by difference-of-concave (DC) programming and the convex-concave procedure (CCP). The actual-power parameterization converts the QoS and power-priority requirements into affine constraints and avoids the bilinear coupling created by independently optimizing total subchannel power and a power-split factor. A Hessian argument proves that the fixed-pair sum rate has the form $F(p)-G(p)$, with F and G concave. Linearizing G gives a tight concave lower-bound surrogate; accepted CCP iterates are therefore non-decreasing in the exact objective under the stated solution conditions, while global optimality is not claimed. A MATLAB R2016b implementation is evaluated using 500 paired Monte Carlo realizations per point. At 100 candidate users, SINR-CCP improves mean sum rate by 2.80% over Gain-CCP, isolating the matching contribution, and by 14.41% over Gain-Heuristic for the complete framework. At 40 dBm, the corresponding gains are 3.95% and 24.02%. The paired 95% confidence intervals remain positive at the reported endpoints, and the numerical audit records monotone accepted-objective traces with negligible affine-constraint residuals. The results support a selective, interference-aware PD-NOMA gain rather than universal superiority over orthogonal access.

Keywords— Power-domain NOMA; SINR-based matching; resource allocation; DC programming; convex-concave procedure; sum-rate maximization

I. INTRODUCTION

Power-domain non-orthogonal multiple access allows two or more users to share a time-frequency resource by superposition coding at the base station and successive interference cancellation at the stronger receiver. This mechanism can improve resource utilization, but the gain is not automatic. A scheduled pair must have a valid decoding order, sufficient channel disparity, adequate power for both users, and a strong receiver capable of decoding the weak-user codeword before cancelling it. A rate-maximizing allocator that ignores these conditions may select an attractive but infeasible assignment..

The literature has established the importance of user pairing, power allocation, and receiver ordering in downlink NOMA [1, 4]. Channel-gain pairing is attractive because it is inexpensive, and fixed power-allocation rules provide a useful baseline. However, channel gain alone does not represent the interference state induced by a candidate pair. SINR-based criteria can reflect the desired signal, intra-pair interference, noise, reference power, and decoding direction simultaneously [5]. At the same time, optimizing pairing and power jointly creates a mixed discrete–continuous problem whose continuous part is non-convex because the weak-user rate contains a fractional SINR.

DC programming provides a natural way to handle this rate structure [6], [7]. Its correct use nevertheless depends on the parameterization. If the total subchannel power and its split factor are treated as independent optimization variables, products of the form $\beta_n P_n$ and $(1-\beta_n)P_n$ obscure curvature and complicate feasibility. The formulation developed here instead optimizes the actual user powers. This choice exposes affine QoS and ordering constraints and permits a direct Hessian proof of the DC decomposition.

The paper makes four bounded contributions:

- A feasibility-screened, pair-aware SINR matching stage that preserves explicit strong/weak roles, user uniqueness, and the joint minimum-power budget.
- An actual-power fixed-pair model in which total power, QoS, optional SIC threshold, power priority, and non-negativity form an affine feasible set.

- A rigorous DC/CCP derivation with a negative-semidefinite Hessian proof, a tangent-bound argument, feasible initialization, exact-objective acceptance, and a stationary-point—not global-optimum—claim.
- A paired Monte Carlo study with controlled ablations that separately identify the value of SINR matching, CCP power optimization, and the complete framework, together with reproducibility and numerical-audit evidence.

The remainder of the paper reviews related methods, presents the system model and optimization problem, develops the two-stage algorithm and its mathematical justification, documents the simulation design, reports the results, and closes with limitations and conclusions.

II. Related Works

A. Pairing and power allocation in PD-NOMA

Early system-level studies demonstrated the potential of downlink NOMA when superposition coding and SIC are combined with opportunistic scheduling [2]. Subsequent analyses showed that user pairing materially changes outage and rate performance [3]. Survey work has organized the broader NOMA and NOMA–MIMO design space around clustering, power allocation, beamforming, interference, and implementation complexity [1], [4]. These results motivate joint reasoning about discrete assignment and continuous power, but they do not make every NOMA schedule preferable to orthogonal access.

Gain-based pairing commonly favours users with dissimilar channel gains. It is simple and often effective, yet its ranking is only indirectly related to the two decoding SINRs. SINR-aware power policies and feasibility conditions more directly express the effect of interference and the SIC order [5]. Matching-theoretic designs can reduce the combinatorial burden of exhaustive pairing, although preferences become pair-dependent when a subchannel evaluates a two-user coalition. The algorithm in this paper is therefore described as a finite pair-aware matching heuristic; it does not claim the classical global stability guarantee of one-to-one Gale–Shapley matching.

B. DC optimization and CCP

DC programming represents a non-convex objective or constraint as the difference of convex or concave components. In NOMA, logarithmic rate identities can expose this structure, and DC methods have been applied to OFDM-based power allocation [7] and energy-efficient resource allocation [6]. CCP replaces the subtracted concave component by its affine first-order upper bound, producing a tractable convex subproblem at each iteration [10]–[12]. The method is local: under regularity and accurate subproblem solution, it approaches a stationary or critical point. It does not certify the global optimum of the original non-convex problem.

C. Recent joint resource-allocation studies

Recent NOMA studies increasingly combine several discrete and continuous decisions. Xie et al. jointly optimized channel assignment, power-allocation factors, and D2D transmit power in a heterogeneous NOMA-D2D network [16]. Xu et al. considered dynamic pairing in a RIS-aided multi-cluster NOMA system and combined Hungarian assignment with successive convex approximation and alternating optimization of beamforming, power, and RIS phases [17]. Zhao et al. developed joint mode selection and power allocation for two-user downlink MISO-NOMA with minimum-rate guarantees [18]. These studies demonstrate the breadth of contemporary NOMA optimization, but their system architectures, objectives, and coupled variables differ from the scalar multicarrier problem addressed here.

Table 1. Positioning against representative recent NOMA resource-allocation studies.

Study	System	Main method	Distinguishing focus
Xie et al. [16]	NOMA-D2D heterogeneous network	Channel/resource assignment and power control	Joint interference-aware allocation in a D2D setting
Xu et al. [17]	RIS-aided multi-cluster NOMA	Hungarian pairing plus SCA/AO	Joint beamforming, power and RIS-phase optimization
Zhao et al. [18]	Two-user downlink MISO-NOMA	Mode selection and parameterized power allocation	QoS-constrained rate-region and fairness trade-offs
This work	Single-cell multicarrier downlink PD-NOMA	Feasibility-screened SINR matching plus actual-power CCP	Matching-only and power-stage ablations on paired realizations, with exact numerical audits

D. Gap addressed

The unresolved issue is not simply whether pairing and power can be optimized jointly. It is whether the contribution of interference-aware matching can be isolated from the power optimizer while maintaining a single, auditable feasibility model. Three elements are therefore treated together here: candidate pairs are screened against minimum power before preference construction; the power optimizer uses actual powers rather than a coupled total-power/split-factor parameterization; and the empirical design uses identical paired channel realizations and a common CCP stage so that matching-only and power-

allocation effects can be measured separately. Table 1 makes this distinction explicit. The resulting contribution is a traceable path from physical feasibility to the reported rate differences, rather than another claim based only on comparison with a weak or differently optimized baseline.

III. SYSTEM MODEL AND PROBLEM FORMULATION

A. Downlink model and ordered users

Consider one base station, N orthogonal subchannels, and K candidate users. At most two users are multiplexed on an active subchannel. Channels are constant during one allocation interval, perfect channel-state information is assumed at the allocator, and ideal SIC is used as the analytical baseline. Let $H_{k,n}=|h_{k,n}|^2/\sigma_n^2$ denote the channel power gain normalized once by the subchannel noise power. For each active pair, user 1 is relabelled as the strong/SIC user and user 2 as the weak user:

$$H_{1,n} \geq H_{2,n} > 0. \tag{1}$$

The actual powers $p_{1,n}$ and $p_{2,n}$ are the primary optimization variables. The total subchannel power $P_n=p_{1,n}+p_{2,n}$ and the strong-user fraction $\beta_n=p_{1,n}/P_n$ are derived reporting quantities only. This distinction removes the bilinear products that arise when P_n and β_n are optimized independently.

B. SINR and achievable rates

With normalized gains, the weak user decodes its own signal while treating the strong-user signal as interference. The strong user first decodes the weak-user codeword and then, after perfect cancellation, decodes its own signal. The three SINRs are

$$\gamma_{2,n} = \frac{p_{2,n}H_{2,n}}{1 + p_{1,n}H_{2,n}}. \tag{2a}$$

$$\gamma_{2\to1,n} = \frac{p_{2,n}H_{1,n}}{1 + p_{1,n}H_{1,n}}. \tag{2b}$$

$$\gamma_{1,n} = p_{1,n}H_{1,n}. \tag{2c}$$

The absence of $p_{2,n}$ from the post-SIC denominator in (2c) is essential. Retaining that term would model residual interference and would contradict the perfect-SIC baseline. The scheduled-user rates are

$$R_{1,n} = B_n \log_2\left(1 + p_{1,n}H_{1,n}\right), \tag{3a}$$

$$R_{2,n} = B_n \log_2\left(1 + \frac{p_{2,n}H_{2,n}}{1 + p_{1,n}H_{2,n}}\right). \tag{3b}$$

C. Affine feasibility conditions

Let $R_{k,n}^{min}$ be the required rate and define the associated SINR target

$$\tau_{k,n} = 2^{R_{k,n}^{min}/B_n} - 1, \qquad k \in \{1,2\}. \tag{4}$$

The strong-user QoS condition and the weak-user QoS condition are equivalent to

$$p_{1,n} \geq \frac{\tau_{1,n}}{H_{1,n}}. \tag{5a}$$

$$p_{2,n} \geq \tau_{2,n}p_{1,n} + \frac{\tau_{2,n}}{H_{2,n}}. \tag{5b}$$

Both are affine in the actual powers. The total-power, priority, and non-negativity conditions are

$$\sum_{n\in\mathcal{N}_a} \left(p_{1,n} + p_{2,n}\right) \leq P_{tot}, \tag{6a}$$

$$p_{2,n} \geq p_{1,n} \tag{6b}$$

where N_a is the set of active paired subchannels. If an independent SIC target $\Gamma_{2,n}^{sIc}$ is required, it also becomes affine:

$$p_{2,n} \geq \Gamma_{2,n}^{\mathrm{SIC}}p_{1,n} + \frac{\Gamma_{2,n}^{\mathrm{SIC}}}{H_{1,n}}. \tag{7}$$

For the ordered-gain perfect-SIC baseline, the function $p_2H/(1+p_1H)$ is non-decreasing in H. Hence $H_{1,n}\geq H_{2,n}$ implies $\gamma_{2\to1,n}\geq\gamma_{2,n}$. Meeting the weak-user rate target therefore supports decodability at the strong receiver when both use the same threshold. A positive SIC margin can be added through (7) for robustness studies.

D. Mixed discrete–continuous objective

The full problem selects at most one ordered pair per subchannel, uses each physical user at most once, and maximizes the sum of (3a) and (3b) subject to (5)–(7). The binary pairing variables make the joint problem combinatorial. Even after the pairs are fixed, the weak-user rate is non-concave in the two powers because it is the logarithm of a fractional SINR. The proposed decomposition therefore separates pair selection from fixed-pair power allocation while preserving a common feasibility model.

IV. PROPOSED TWO-STAGE METHOD

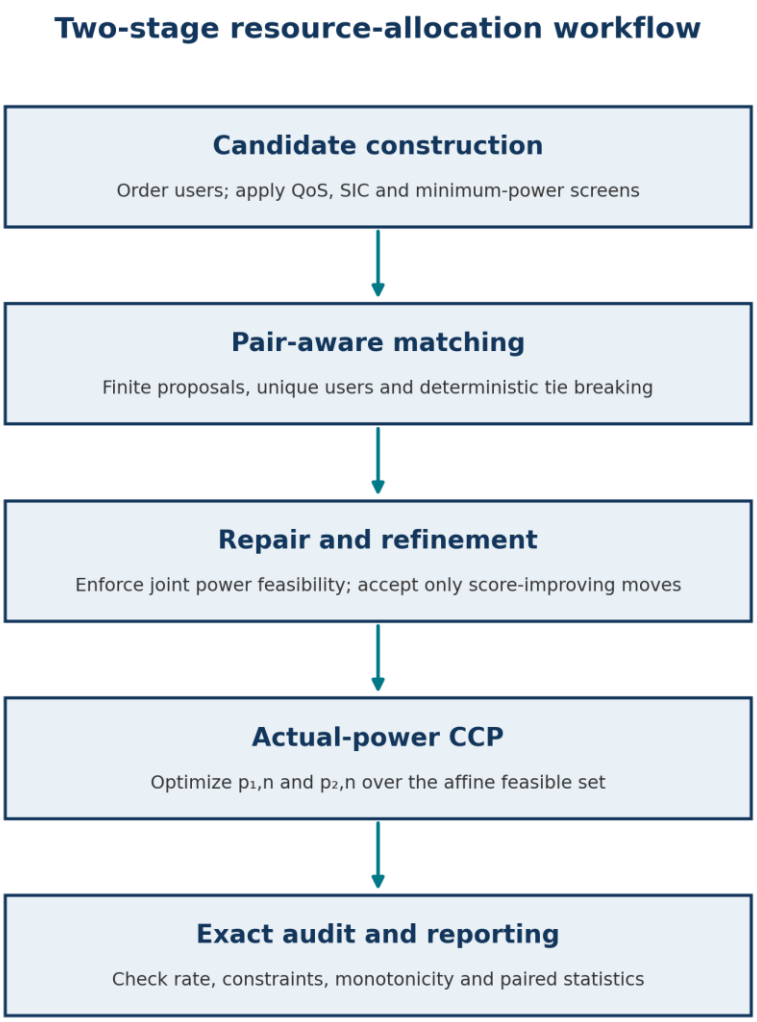


Fig. 1. Proposed two-stage resource-allocation workflow.

A. Feasibility-screened SINR candidate construction

For each subchannel, every unordered user pair is relabelled by (1). With $\tau_{1,n}$ and $\tau_{2,n}$ from (4), the minimum strong-user power is $q_1=\tau_{1,n}/H_{1,n}$ and the minimum weak-user power is $q_2=\max\{q_1, \tau_{2,n}q_1+\tau_{2,n}/H_{2,n}\}$. A pair is removed if q_1+q_2 exceeds the total budget, if its gains are invalid, or if its reference SIC condition fails. This screen prevents a high-ranking but individually impossible pair from entering the preference lists.

The remaining pairs are scored at a fixed reference allocation P_{tot}/N with strong-user fraction $\beta_0=0.20$. SINR scoring uses the sum of the two reference rates, whereas the gain comparator uses $\log(1+H_1)+\log(1+H_2)$. The reference allocation only constructs preferences; it is not the final optimized power.

B. Finite matching, repair, and local refinement

Users propose to eligible subchannels according to scheme-specific preferences. A subchannel holds at most two users and retains the feasible held pair with the largest score, using minimum required power and lexicographic indices to break ties. Each user proposes to each eligible subchannel at most once, so the proposal phase terminates after at most KN proposals. Because a subchannel evaluates a pair rather than an independent user, the resulting procedure is a pair-aware deferred-acceptance heuristic and is not presented as a proof of classical global stability.

After proposals terminate, the selected minimum powers are summed. If the joint total is infeasible, the selected pair with the smallest score-to-required-power ratio is banned and matching is rerun. For SINR matching, a deterministic local-refinement stage then considers feasible pair additions, one-user replacements, pair relocations, and inter-subchannel swaps. A move is accepted only if it preserves user uniqueness and joint feasibility and strictly increases the fixed-reference SINR score. The procedure stops at a local score-stable state or after 25 rounds.

Algorithm 1. Feasibility-screened pair-aware matching.

Step	Stage-1 operation
1	Normalize gains once by the subchannel noise power and order every candidate pair.
2	Compute q_1 and q_2; reject pairs that violate individual power or reference-SIC feasibility.
3	Construct SINR- or gain-based user and pair preferences with deterministic tie breaking.
4	Run finite proposals while enforcing one subchannel per user and at most two held users.
5	Repair joint minimum-power infeasibility by banning the least efficient selected pair.
6	For SINR matching, accept only feasible score-improving additions, replacements, relocations, or swaps.

C. Exact DC decomposition for fixed pairs

For fixed pairs, rewrite the weak-user rate as a difference of logarithms:

$$R_{2,n} = B_n \log_2\left(1 + \left(p_{1,n} + p_{2,n}\right)H_{2,n}\right) - B_n \log_2\left(1 + p_{1,n}H_{2,n}\right) \tag{8}$$

For $\mathbf{p}_n=[p_{1,n},p_{2,n}]^T$, define

$$F_n(\mathbf{p}_n) = B_n \log_2\left(1 + p_{1,n}H_{1,n}\right) + B_n \log_2\left(1 + \left(p_{1,n} + p_{2,n}\right)H_{2,n}\right) \tag{9a}$$

$$G_n(\mathbf{p}_n) = B_n \log_2\left(1 + p_{1,n}H_{2,n}\right) \tag{9b}$$

$$R_{\Sigma}(\mathbf{p}) = F(\mathbf{p}) - G(\mathbf{p}) \tag{9c}$$

where $F=\Sigma_n F_n$ and $G=\Sigma_n G_n$. The decomposition follows algebraically from (8); it is not an approximation. Define positive scalars $a_{1,n}$ and $a_{2,n}$ as in the Appendix. The Hessian of F_n is

$$\nabla^2 F_n = -a_{1,n}\begin{bmatrix}1 & 0\\ 0 & 0\end{bmatrix} - a_{2,n}\begin{bmatrix}1 & 1\\ 1 & 1\end{bmatrix} \tag{10}$$

For any vector $\mathbf{v}=[v_1,v_2]^T$,

$$\mathbf{v}^T\nabla^2 F_n\mathbf{v} = -a_{1,n}v_1^2 - a_{2,n}(v_1+v_2)^2 \le 0 \tag{11}$$

so F_n is jointly concave. Similarly, the Hessian of G_n is negative semidefinite:

$$\nabla^2 G_n = -a_{3,n}\begin{bmatrix}1 & 0\\ 0 & 0\end{bmatrix} \preccurlyeq 0 \tag{12}$$

Therefore F and G are concave and (9c) is a valid difference-of-concave representation. Notice that negative individual Hessian entries alone would not prove concavity; the quadratic-form or eigenvalue condition in (11) is required.

D. CCP update, feasibility, and convergence statement

At iteration t, concavity gives the global affine upper bound

$$G(\mathbf{p}) \le \hat{G}\left(\mathbf{p};\mathbf{p}^{(t)}\right) = G\left(\mathbf{p}^{(t)}\right) + \nabla G\left(\mathbf{p}^{(t)}\right)^T\left(\mathbf{p} - \mathbf{p}^{(t)}\right) \tag{13}$$

Consequently, $F(\mathbf{p})-\hat{G}(\mathbf{p};\mathbf{p}^{(t)})$ is a concave global lower bound of the exact objective $F(\mathbf{p})-G(\mathbf{p})$, and it is tight at $\mathbf{p}^{(t)}$. Each CCP step maximizes this surrogate over the unchanged affine feasible set. A feasible initializer is formed from the minimum QoS powers:

$$p_{1,n}^{(0)} = \frac{\tau_{1,n}}{H_{1,n}} \tag{14a}$$

$$p_{2,n}^{(0)} = \max\left\{p_{1,n}^{(0)},\ \tau_{2,n}p_{1,n}^{(0)} + \frac{\tau_{2,n}}{H_{2,n}}\right\} \tag{14b}$$

Any remaining budget is initially distributed to weak-user powers using deterministic channel-based weights. Each numerical candidate is audited using the exact rates and all affine residuals. If solver tolerances produce a small exact-objective decrease, a convex-combination damping step is attempted; otherwise, the candidate is rejected. Because the previous iterate is feasible for the next subproblem and the surrogate is tight there, exact surrogate maximization yields a non-decreasing accepted exact-objective sequence. The total-power constraint bounds the feasible set. Under standard CCP regularity and subproblem-solution conditions, accumulation points are stationary or critical; global optimality is not guaranteed [10]–[12].

Algorithm 2. Actual-power CCP allocation.

Step	Stage-2 operation
1	Construct a feasible actual-power initializer from (14).
2	Evaluate exact F, G, sum rate, and all constraint residuals.
3	Form the affine upper bound $\hat{G}$ at the current feasible power vector.
4	Solve the convex surrogate problem over the unchanged affine feasible set.
5	Audit the exact objective and constraints; damp or reject an unacceptable candidate.
6	Stop when relative exact-objective improvement is at most 10^{-4} or after 50 iterations.

E. Computational structure

Candidate enumeration requires $O(NK^2)$ pair checks. The proposal phase has at most KN user–subchannel proposals, while local refinement is deliberately bounded by 25 rounds. If N_a pairs are active, the CCP subproblem contains $2N_a$ continuous variables and affine constraints. Thus, exhaustive enumeration of all global pairings and powers is avoided; the principal numerical cost is the repeated convex surrogate solution. The reported runtime is implementation- and hardware-dependent and is used only as a computational profile, not as proof of real-time deployment.

V. SIMULATION METHODOLOGY

A. Channel and experiment configuration

The corrected model was implemented in MATLAB R2016b using Optimization Toolbox. Users are drawn uniformly by area in an annulus, large-scale loss follows a log-distance model, and each user–subchannel link experiences independent Rayleigh fading. Gains are normalized once by the calculated subchannel noise power. The two sweeps are separate experiments: K=10,20,…,100 at 40 dBm, and P_{tot}=0,5,…,40 dBm at K=20. Each point uses 500 paired realizations with the same channel sample supplied to every scheme.

Table 2. Reference simulation configuration.

Parameter	Value
Cell / minimum distance	500 m / 35 m
Path loss at 1 m / exponent	30 dB / 3.5
Carrier frequency	2 GHz
Noise PSD / noise figure	−174 dBm/Hz / 7 dB
Total bandwidth / subchannels	1.44 MHz / 8
Subchannel bandwidth	180 kHz
Minimum spectral efficiency	0.5 bit/s/Hz
Reference strong-user fraction	0.20 (Stage 1 only)
SIC model / margin	Perfect / 0
User sweep	K=10:10:100 at 40 dBm
Power sweep	0:5:40 dBm at K=20
Trials / base seed	500 / 271828
CCP cap / tolerance	50 / 10^{-4}

B. Controlled comparison schemes

Table 3. Controlled schemes and interpretation.

Scheme	Purpose
SINR-CCP	Proposed matching, repair/refinement, and CCP power optimization.
Gain-CCP	Gain-based matching with the identical CCP optimizer; isolates Stage 1.
SINR-Heuristic	Proposed matching with feasible deterministic heuristic powers; isolates Stage 2.
Gain-Heuristic	Gain matching and heuristic powers; complete-framework comparator.
Random-CCP	Random feasible preferences with the identical CCP optimizer.
OMA	Greedy unique-user/subchannel assignment with equal power; contextual reference.

The primary matching claim is based on SINR-CCP versus Gain-CCP because both use the same power optimizer. SINR-CCP versus SINR-Heuristic measures the value of Stage 2. SINR-CCP versus Gain-Heuristic measures the complete two-stage framework. These comparisons must not be interchanged. OMA is contextual because it schedules one user per subchannel with a different multiplexing structure and is not a globally optimized OMA bound.

C. Statistical reporting and software verification

For a paired comparison, the trial-level difference $d_m = R_m^A - R_m^B$ is computed on the same realization. The mean difference is reported with the pointwise 95% confidence interval $\bar{d} \pm t_{0.975,M-1} s_d/\sqrt{M}$. Pairing removes much of the channel-realization variance and directly tests whether one algorithm is better on the same sample. Win rate is the fraction of realizations for which $d_m > 0$.

The implementation stores run configuration, random seeds, summary CSV files, exact-objective traces, constraint residuals, and a MAT file containing realization-level data. Ten regression tests verify dBm conversion, noise normalization, the DC identity and tangent direction, minimum QoS powers, role ordering, user uniqueness, local refinement, heuristic feasibility, CCP feasibility/monotonicity, and limiting rate cases. The acceptance audit independently recomputes rates and constraint residuals after every accepted allocation.

All schemes at a given operating point use the same channel realization, noise sample, QoS targets, total-power budget, and stopping tolerances. Consequently, SINR-CCP versus Gain-CCP changes only the matching rule; SINR-CCP versus SINR-Heuristic changes only the power-allocation stage. This controlled design prevents the overall framework gain from being incorrectly attributed to either stage alone.

VI. RESULTS AND DISCUSSION

A. Candidate-user sweep

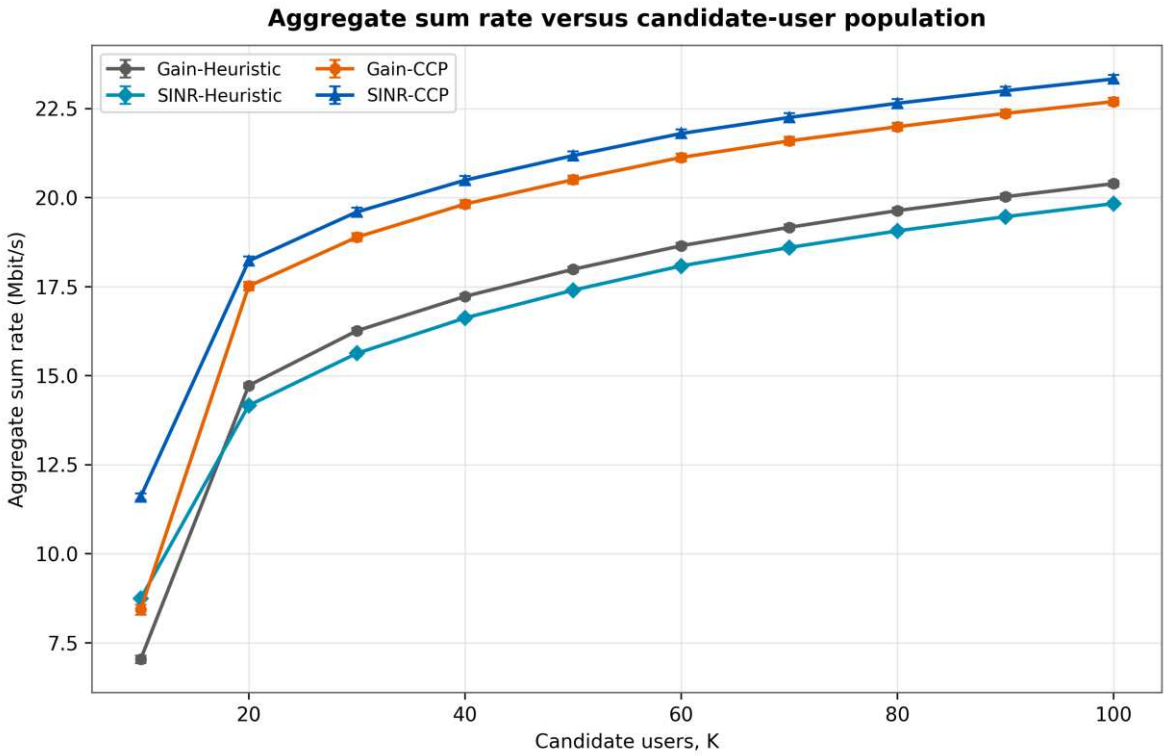


Fig. 2. Aggregate sum rate versus candidate-user population. Error bars are pointwise 95% confidence intervals over 500 paired realizations.

Figure 2 shows multiuser-diversity growth followed by a slower increase as the eight subchannels become fully loaded. At K=100, SINR-CCP reaches 23.333 Mbit/s, compared with 22.697 Mbit/s for Gain-CCP, 20.394 Mbit/s for Gain-Heuristic, and 19.833 Mbit/s for SINR-Heuristic. The controlled matching gain over Gain-CCP is therefore 2.80%. The full framework improves on Gain-Heuristic by 14.41%, while CCP improves the SINR-matched heuristic allocation by 17.65%.

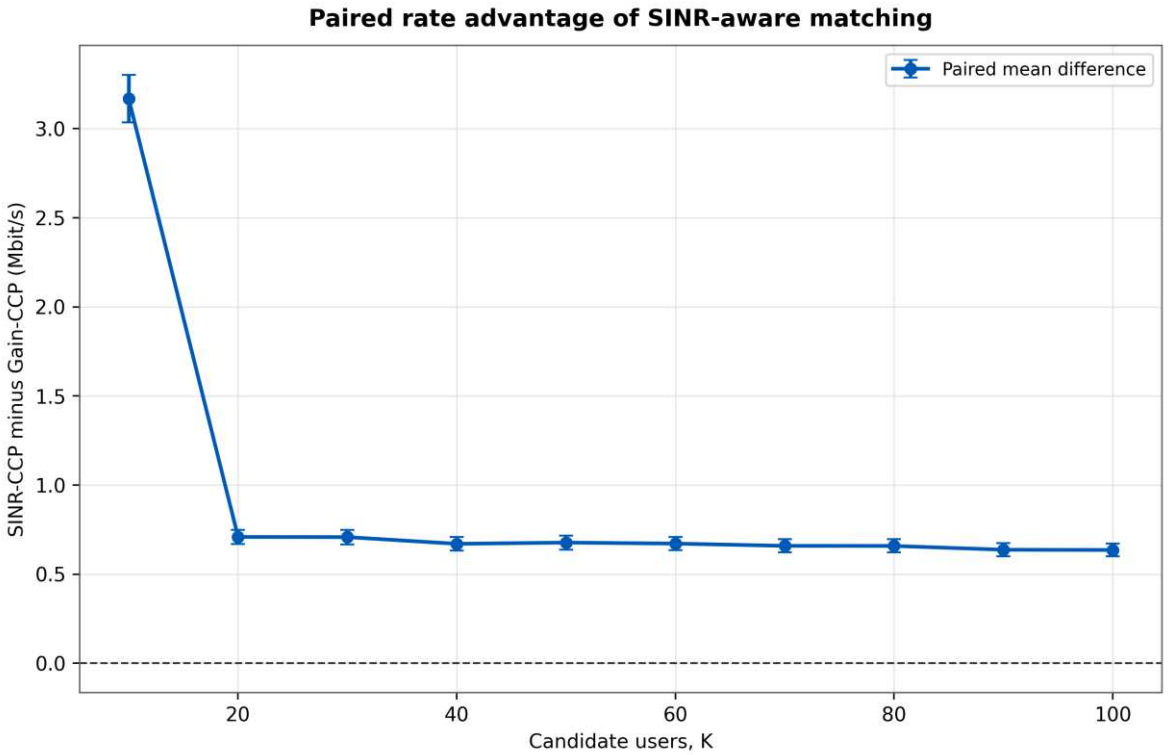


Fig. 3. Paired mean sum-rate difference, SINR-CCP minus Gain-CCP, versus candidate-user population.

Figure 3 isolates the matching contribution using a common CCP stage. The paired mean difference is positive at every user-count point. At K=100, it is 0.636 Mbit/s with a 95% confidence interval of [0.600, 0.671] Mbit/s and a 96.8% trial win rate. The larger improvement at K=10 reflects the additional effect of feasibility and service: the SINR procedure forms feasible pairs more consistently in the lightly populated candidate set. At larger K, both methods usually fill all eight pairs, and the remaining difference reflects pair quality rather than pair count.

B. Transmit-power sweep and OMA context

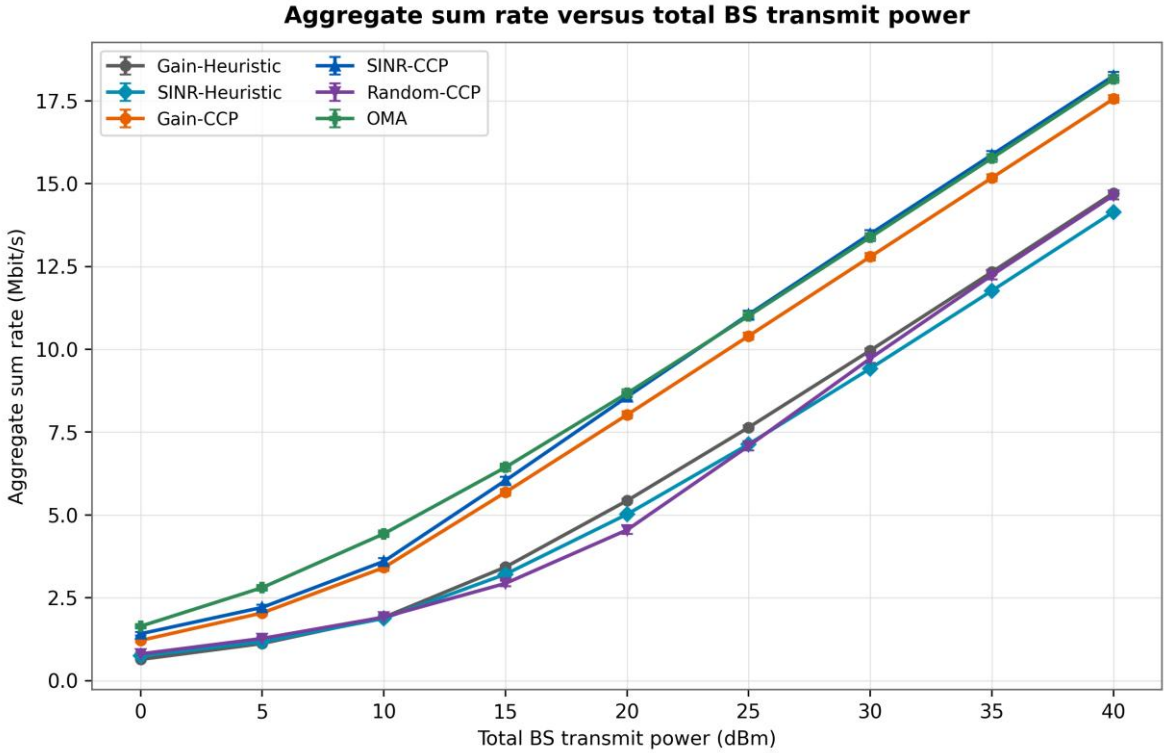


Fig. 4. Aggregate sum rate versus total base-station transmit power for the proposed method and five benchmarks.

Figure 4 shows that SINR-CCP remains above Gain-CCP across the sweep, but OMA is stronger at low power. This is a meaningful boundary: when power is scarce, supporting two QoS-constrained users on one subchannel can be less rate-efficient than serving one strong user. As power and pair capacity increase, the proposed NOMA method becomes competitive. At 40 dBm, SINR-CCP achieves 18.249 Mbit/s; Gain-CCP, Gain-Heuristic, SINR-Heuristic, Random-CCP, and the stated OMA reference achieve 17.556, 14.715, 14.145, 14.645, and 18.157 Mbit/s, respectively. Thus, the proposed scheme is only 0.50% above this OMA reference at the endpoint and should not be described as universally superior to OMA.

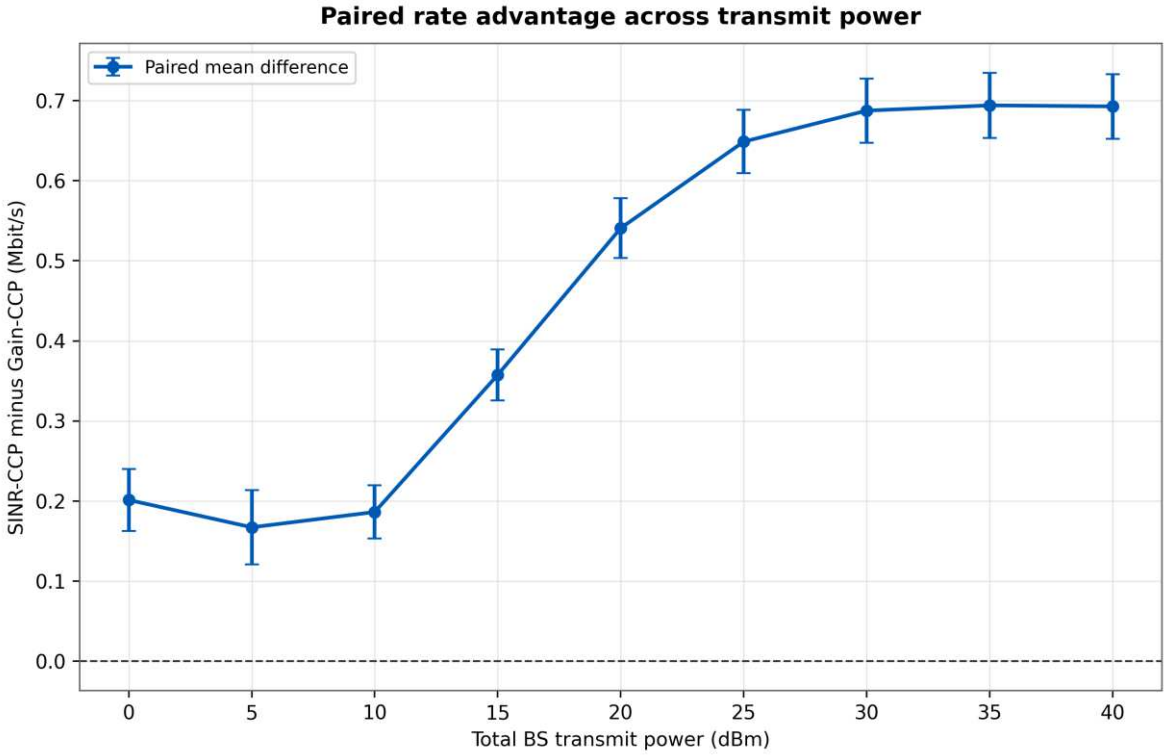


Fig. 5. Paired mean sum-rate difference, SINR-CCP minus Gain-CCP, versus transmit power.

At 40 dBm, the matching-only advantage is 0.693 Mbit/s, with a 95% confidence interval of [0.652, 0.733] Mbit/s and a 97.0% win rate. This equals a 3.95% relative improvement over Gain-CCP. The complete framework improves on Gain-Heuristic by 3.534 Mbit/s or 24.02%, while CCP improves on SINR-Heuristic by 4.104 Mbit/s or 29.01%. At 0–10 dBm, the smaller pair counts and QoS screen influence both means; comparisons there describe the entire feasibility policy as well as ranking quality.

Table 4. Controlled endpoint comparisons.

Endpoint	Paired comparison	Mean difference [95% CI]	Gain	Win
K=100	SINR-CCP − Gain-CCP	0.636 [0.600, 0.671] Mbit/s	2.80%	96.8%
K=100	SINR-CCP − Gain-Heuristic	2.939 [2.865, 3.013] Mbit/s	14.41%	100%
K=100	SINR-CCP − SINR-Heuristic	3.500 [3.416, 3.584] Mbit/s	17.65%	100%
40 dBm	SINR-CCP − Gain-CCP	0.693 [0.652, 0.733] Mbit/s	3.95%	97.0%
40 dBm	SINR-CCP − Gain-Heuristic	3.534 [3.445, 3.623] Mbit/s	24.02%	100%
40 dBm	SINR-CCP − SINR-Heuristic	4.104 [4.002, 4.206] Mbit/s	29.01%	100%

C. SINR and active-user rate distribution

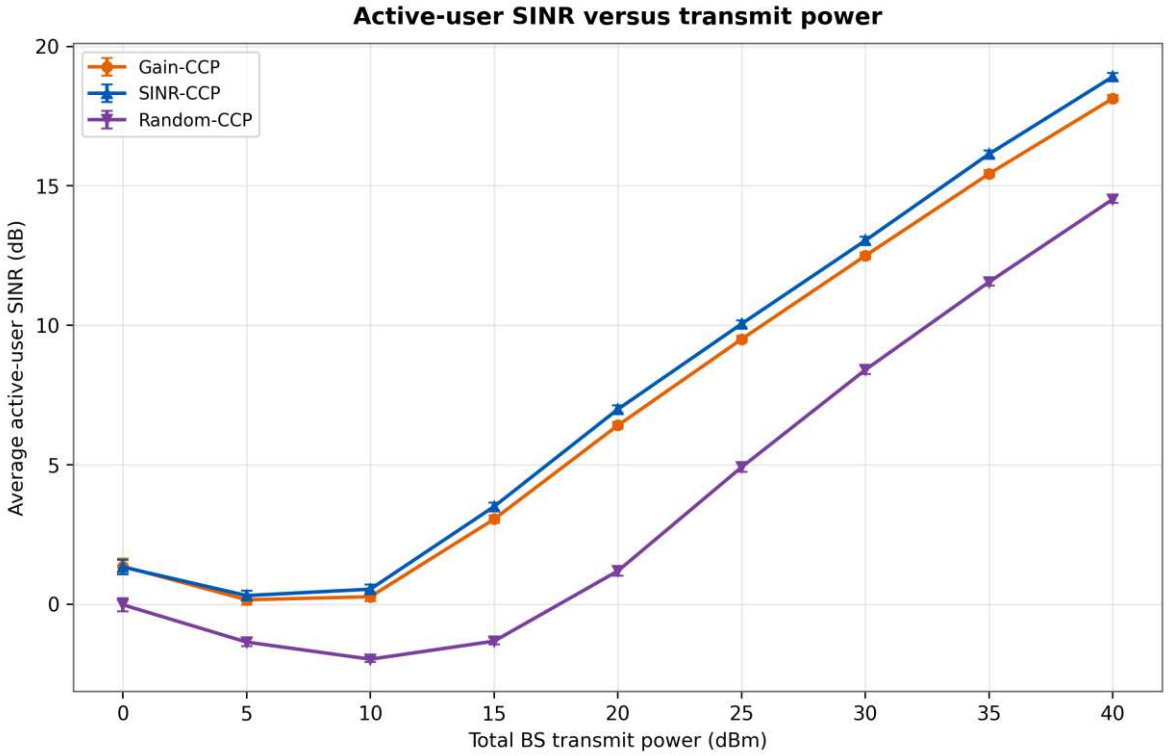


Fig. 6. Average active-user SINR versus total transmit power.

The active-user SINR in Fig. 6 increases once enough power is available to fill the eight NOMA pairs. At 40 dBm, the mean active-user SINR is 18.92 dB for SINR-CCP, 18.14 dB for Gain-CCP, and 14.52 dB for Random-CCP. This supports the interpretation that the proposed matching stage creates a more favourable interference and decoding structure. The quantity is averaged over scheduled active users; it is not a population-wide coverage metric.

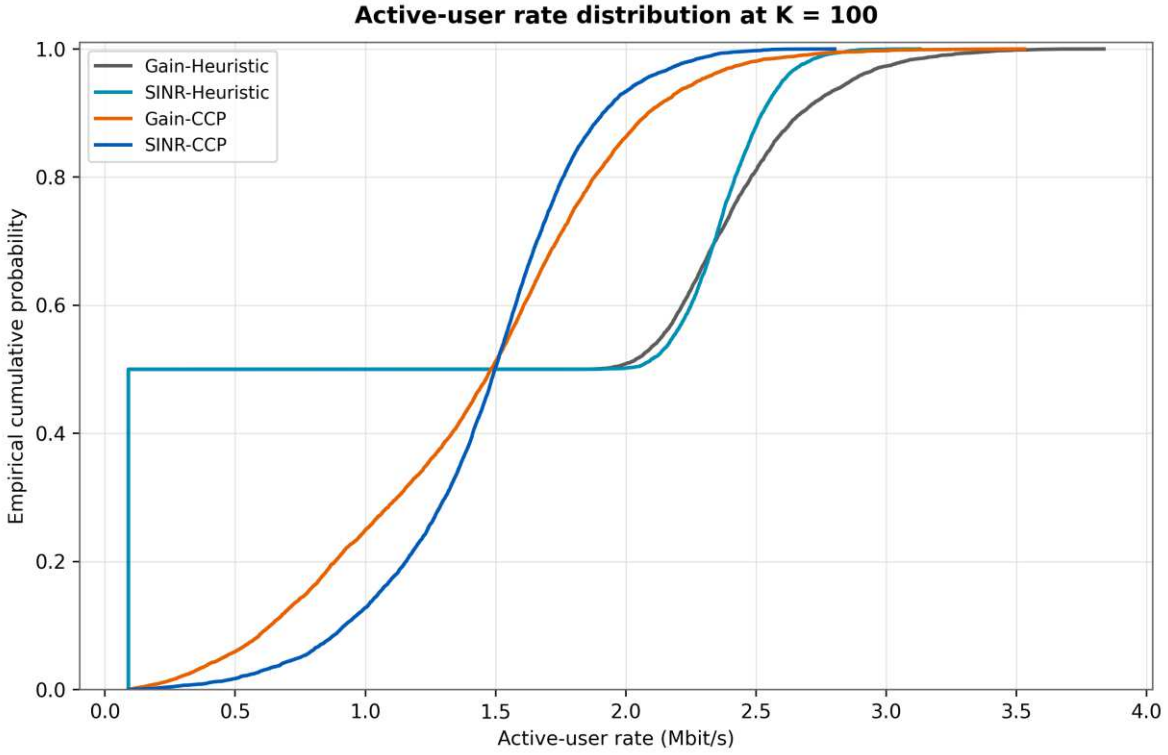


Fig. 7. Empirical CDF of positive active-user rates at K=100.

At K=100, every NOMA scheme can schedule at most 16 of the 100 candidates, so unscheduled zeros dominate population-wide fairness and outage. Figure 7 therefore conditions on positive active-user rates and must be read alongside the service fraction. SINR-CCP has a median active-user rate of 1.497 Mbit/s; its 10th and 90th percentiles are 0.920 and 1.912 Mbit/s.

Gain-CCP has a similar median of 1.483 Mbit/s but a wider lower tail, with a 10th percentile of 0.636 Mbit/s. This pattern suggests that the SINR-aware matching stage improves the weaker part of the scheduled-user distribution while maintaining aggregate rate.

D. Feasibility, convergence, and runtime

The power sweep is nearly fully feasible at the lowest points and fully feasible for SINR-CCP from 15 dBm onward. The mean active-pair count increases from approximately 2.69 at 0 dBm to all eight pairs at 15 dBm. This is expected from the QoS screen and should not be misinterpreted as numerical failure. Across the two main sweeps, the three CCP schemes generated 28,500 trial traces. Of these, 28,427 feasible runs converged under the declared stopping rule; the maximum recorded affine-constraint violation was 3.55×10^{-15} W, and every accepted exact-objective trace was non-decreasing within tolerance.

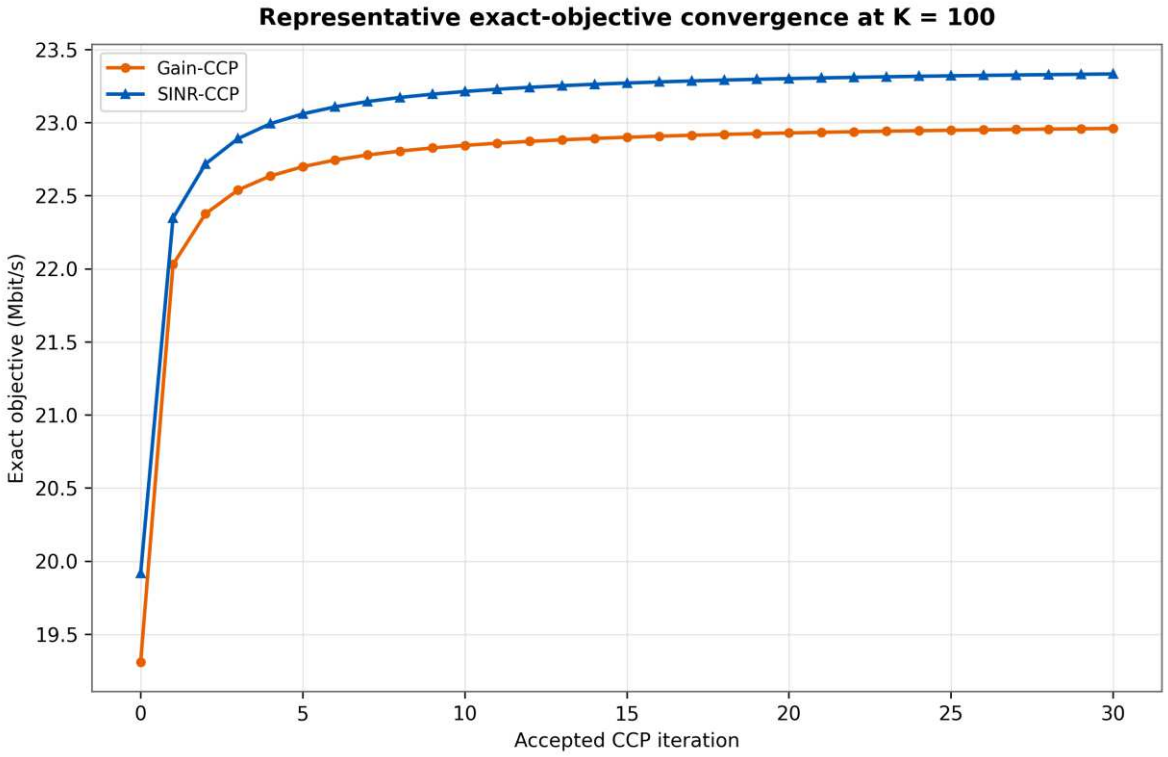


Fig. 8. Representative exact-objective convergence at K=100.

Figure 8 illustrates a representative accepted-objective trace. Rapid early improvement is followed by smaller increments, and both schemes approach their stopping thresholds in roughly 30 accepted iterations. The trace validates the implemented monotonic acceptance logic for this realization; it does not prove global optimality or establish that every realization converges at the same speed.

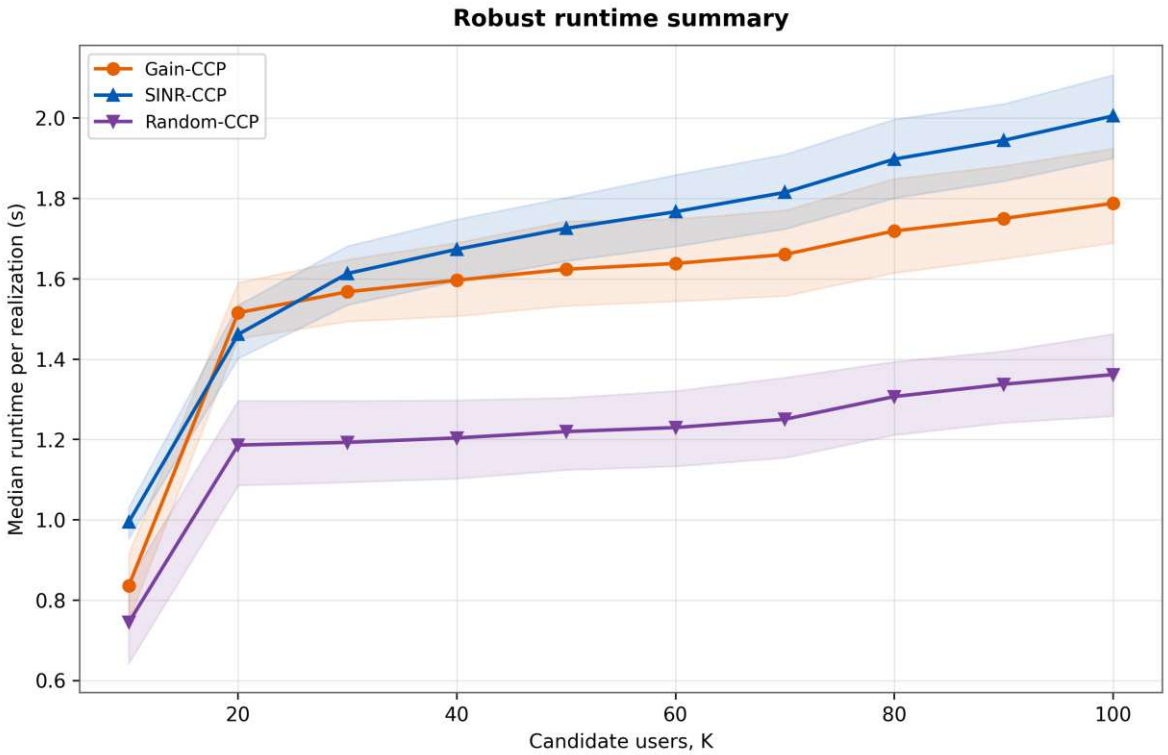


Fig. 9. Median per-realization runtime versus candidate-user population; shading shows the interquartile range.

At K=100, median runtime is 2.006 s for SINR-CCP, 1.788 s for Gain-CCP, and 1.362 s for Random-CCP in the research implementation. The SINR method incurs extra matching and refinement work. Medians and interquartile bands are reported because a single external interruption produced a non-representative timing record. These values demonstrate computational tractability for offline study, not real-time base-station readiness.

Table 5. Numerical verification evidence.

Audit item	Recorded evidence
Paired Monte Carlo	500 identical channel realizations per point and scheme.
CCP traces	28,500 stored traces; 28,427 feasible runs converged.
Constraint audit	Maximum recorded affine violation: 3.55×10^{-15} W.
Monotonicity	All accepted exact-objective traces non-decreasing within tolerance.
Regression tests	10/10 tests passed, including DC identity, tangent bound and role checks.
Reproducibility	Manifest, seed, CSV summaries, MAT data, figures and source files retained.

VII. LIMITATIONS AND IMPLICATIONS

The evidence supports a specific claim: under the declared single-cell, two-user, perfect-CSI, perfect-SIC configuration, feasibility-screened SINR matching improves mean sum rate over gain matching when both use the same CCP optimizer. It also supports the value of the CCP power stage relative to the declared heuristic allocation. The study does not establish global optimality, universal NOMA superiority, real-time readiness, or robustness to residual SIC, mobility, multi-cell interference, and channel-estimation error.

The OMA comparison is deliberately contextual. The baseline greedily selects unique user–subchannel assignments and divides power equally; it is not an optimized OMA upper bound. OMA is superior at low power in the tested configuration, and at 40 dBm the difference from SINR-CCP is small. This reinforces the practical need for access-mode selection rather than forcing NOMA in every channel state.

The reference strong-user fraction influences Stage-1 preference scores but is not constrained to be the final split. Moreover, the study does not include a global optimum for the full mixed discrete–continuous problem; the controlled Gain-CCP ablation is the appropriate basis for the matching claim, while the random, heuristic, and OMA schemes provide complementary context rather than optimality certificates. Future work should examine sensitivity to the reference split, positive SIC margins, residual-interference models, unequal QoS targets, load-adaptive numbers of users per subchannel, multi-cell coordination, and exhaustive or globally bounded solutions for small instances. A hardware-aware implementation would also require compiled solvers, latency profiling, and channel-estimation overhead.

VIII. CONCLUSION

This paper developed a two-stage downlink PD-NOMA allocator that connects physical feasibility, pair-aware SINR matching, and actual-power CCP optimization. The actual-power parameterization makes QoS, priority, total-power, and optional SIC-threshold constraints affine. Rewriting the weak-user rate exposes a valid difference-of-concave objective, and the negative-semidefinite Hessian proof plus tangent-bound argument justifies the CCP surrogate. Feasible initialization and exact-objective auditing protect the implementation from silent constraint or monotonicity errors.

The controlled results distinguish the contributions of the two stages. At K=100, SINR-aware matching improves on gain matching by 2.80% under a shared CCP optimizer, while the complete framework improves on gain matching with heuristic powers by 14.41%. At 40 dBm, the corresponding improvements are 3.95% and 24.02%. Positive paired confidence intervals and high win rates support these comparisons. The correct conclusion is therefore bounded: interference-aware, feasibility-screened matching provides a reproducible rate advantage within the tested PD-NOMA model, while broader deployment claims require further validation.

Author Contributions: In this article, M.H., M.B.R. and S.M.M. contributed to the conceptualization of the study. M.H. prepared the original draft of the manuscript and visualized the findings. M.B.R., S.M.M, and A.B.M supervised the study and provided critical feedback on the manuscript. The manuscript has been reviewed and edited by M.H. All authors have read and agreed to the published version of the manuscript.

Acknowledgement: Not applicable.
Funding: This work is supported and funded by a Telekom Malaysia Research & development (TMR&D) grant, RDTC: 241126, MMUE/240081, TM, Malaysia.
Institutional Review Board Statement: Not applicable.
Informed Consent Statement: Not applicable.
Data Availability Statement: All the data are available in the paper.

REFERENCES

[1] M. Halabouni, M. B. Roslee, S. Mitani, O. Abuajwa, A. Osman, F. Z. binti Ali, and A. Waseem, "NOMA-MIMO in 5G network: A detailed survey on enhancing data rate," PeerJ Computer Science, vol. 11, e2388, 2025, doi: 10.7717/peerj-cs.2388.

[2] Y. Saito, A. Benjebbour, Y. Kishiyama, and T. Nakamura, "System-level performance evaluation of downlink non-orthogonal multiple access (NOMA)," in Proc. IEEE PIMRC, 2013, pp. 611–615, doi: 10.1109/PIMRC.2013.6666209.

[3] Z. Ding, P. Fan, and H. V. Poor, "Impact of user pairing on 5G nonorthogonal multiple-access downlink transmissions," IEEE Trans. Veh. Technol., vol. 65, no. 8, pp. 6010–6023, 2016, doi: 10.1109/TVT.2015.2480766.

[4] L. Dai, B. Wang, Y. Yuan, S. Han, C.-L. I, and Z. Wang, "Non-orthogonal multiple access for 5G: Solutions, challenges, opportunities, and future research trends," IEEE Commun. Surveys Tuts., vol. 20, no. 3, pp. 2294–2323, 2018, doi: 10.1109/COMST.2018.2835558.

[5] M. W. Baidas, E. Alsusa, and K. A. Hamdi, "Performance analysis and SINR-based power allocation strategies for downlink NOMA networks," IET Commun., vol. 14, no. 5, pp. 723–735, 2020, doi: 10.1049/iet-com.2018.6112.

[6] F. Fang, H. Zhang, J. Cheng, and V. C. M. Leung, "Energy-efficient resource allocation for downlink non-orthogonal multiple access network," IEEE Trans. Commun., vol. 64, no. 9, pp. 3722–3732, 2016, doi: 10.1109/TCOMM.2016.2594759.

[7] P. Parida and S. S. Das, "Power allocation in OFDM based NOMA systems: A DC programming approach," in Proc. IEEE GLOBECOM Workshops, 2014, pp. 1026–1031, doi: 10.1109/GLOCOMW.2014.7063568.

[8] O. Abuajwa, M. B. Roslee, and Z. B. Yusoff, "Simulated annealing for resource allocation in downlink NOMA systems in 5G networks," Applied Sciences, vol. 11, no. 10, 4592, 2021, doi: 10.3390/app11104592.

[9] M. W. Baidas, M. S. Bahbahani, E. Alsusa, K. A. Hamdi, and Z. Ding, "Joint D2D group association and channel assignment in uplink multi-cell NOMA networks: A matching-theoretic approach," IEEE Trans. Commun., vol. 67, no. 12, pp. 8771–8785, 2019, doi: 10.1109/TCOMM.2019.2944142.

[10] T. Lipp and S. Boyd, "Variations and extension of the convex–concave procedure," Optimization and Engineering, vol. 17, no. 2, pp. 263–287, 2016, doi: 10.1007/s11081-015-9294-x.

[11] H. A. Le Thi and T. Pham Dinh, "DC programming and DCA: Thirty years of developments," Mathematical Programming, vol. 169, no. 1, pp. 5–68, 2018, doi: 10.1007/s10107-018-1235-y.

[12] A. L. Yuille and A. Rangarajan, "The concave-convex procedure," Neural Computation, vol. 15, no. 4, pp. 915–936, 2003, doi: 10.1162/08997660360581958.

[13] A. Akbar, S. Jangsher, and F. A. Bhatti, "NOMA and 5G emerging technologies: A survey on issues and solution techniques," Computer Networks, vol. 190, 107950, 2021, doi: 10.1016/j.comnet.2021.107950

[14] MS. M. R. Islam, N. Avazov, O. A. Dobre, and K.-S. Kwak, “Power-domain non-orthogonal multiple access (NOMA) in 5G systems: Potentials and challenges,” IEEE Commun. Surveys Tuts., vol. 19, no. 2, pp. 721–742, 2017, doi: 10.1109/COMST.2016.2621116.

[15] M. Zeng, A. Yadav, O. A. Dobre, G. I. Tsiropoulos, and H. V. Poor, “Capacity comparison between MIMO-NOMA and MIMO-OMA with multiple users in a cluster,” IEEE J. Sel. Areas Commun., vol. 35, no. 10, pp. 2413–2424, 2017, doi: 10.1109/JSAC.2017.2725879.

[16]] J. Xie, L. Li, and C. Li, “A joint resource optimization allocation algorithm for NOMA-D2D communication,” IET Commun., vol. 18, no. 6, pp. 398–408, 2024, doi: 10.1049/cmu2.12741.

[17] S. Xu, S. Wu, and Y. Zheng, “Joint dynamic user pairing and resource allocation for RIS-aided multi-cluster NOMA networks,” Phys. Commun., vol. 68, art. 102595, 2025, doi: 10.1016/j.phycom.2024.102595.

[18] Z. Zhao, D. Wang, H. Zhang, and X. Huang, “Joint mode selection and resource allocation to flexibly guarantee quality of service for downlink MISO-NOMA systems,” J. King Saud Univ. Comput. Inf. Sci., vol. 36, art. 101913, 2024, doi: 10.1016/j.jksuci.2024.101913.

APPENDIX A

Convexity of $g\ (\beta_n)$

We consider the rate term for the weak user (user 2) in power-domain NOMA, given as a function of the power proportion $\beta_n \in \{0,1\}$;

$$g\ (\beta_n) = -B_{2,n}.\log_2\left(1 + \frac{(1-\beta_n)P_nH_{2,n}}{1+\beta_nP_nH_{2,n}}\right)$$

We define

$$\varphi\ (\beta_n) = \frac{(1-\beta_n)P_nH_{2,n}}{1+\beta_nP_nH_{2,n}}$$

Then

$$g\ (\beta_n) = -B_{2,n}.\log_2\big(1+\varphi\ (\beta_n)\big)$$

- The first derivative:

We Apply the chain rule to differentiate $g\ (\beta_n)$:

$$g'\ (\beta_n) = -B_{2,n}.\frac{1}{\ln(2)}\cdot\frac{\varphi'\ (\beta_n)}{1+\varphi'\ (\beta_n)}$$

Now compute $\varphi'\ (\beta_n)$ using quotient rule:

Let numerator $N\ (\beta_n) = (1-\beta_n)P_nH_{2,n}$
Let denominator $D\ (\beta_n) = 1+\beta_nP_nH_{2,n}$
Then:

$$\varphi'\ (\beta_n) = \frac{N'\ (\beta_n)D\ (\beta_n) - N\ (\beta_n)\ D'\ (\beta_n)}{(D\ (\beta_n))^2}$$

Now:

$$N'\ (\beta_n) = -P_nH_{2,n}$$

$$D'\ (\beta_n) = P_nH_{2,n}$$

Now $\varphi'\ (\beta_n)$ becomes:

$$\varphi'\ (\beta_n) = \frac{-P_nH_{2,n}\big(1+\beta_nP_nH_{2,n}\big) - (1-\beta_n)P_nH_{2,n}.P_nH_{2,n}}{(1+\beta_nP_nH_{2,n})^2}$$

Simplify numerator:

$$\varphi'\ (\beta_n) = \frac{-P_nH_{2,n}\big(1+\beta_nP_nH_{2,n}\big) - (1-\beta_n){P_n}^2{H_{2,n}}^2}{(1+\beta_nP_nH_{2,n})^2}$$

So:

$$g'\ (\beta_n) = -\frac{B_{2,n}}{\ln(2)}\cdot\frac{\varphi'\ (\beta_n)}{1+\varphi'\ (\beta_n)}$$

This gives the slope of the weak user's rate with respect to β_n. It's negative, which reflects the rate decreasing as more power goes to the stronger user.

- The second derivative:

  We Apply product and chain rule to differentiate $g'(\beta_n)$ again;

$$g''(\beta_n) = -\frac{B_{2,n}}{\ln(2)} \cdot \left\{ \frac{d}{d\beta_n} \left(\frac{\varphi'(\beta_n)}{1+\varphi(\beta_n)} \right) \right\}$$

We define the inner derivative as:

$$\frac{d}{d\beta_n} \left(\frac{\varphi'(\beta_n)}{1+\varphi(\beta_n)} \right) = \frac{\varphi'(1+\varphi) - (\varphi')^2}{(1+\varphi)^2}$$

Now we again apply the quotient rule to $\varphi'(\beta_n)$

$$\varphi'(\beta_n) = \frac{\mathrm{A}(\beta_n)}{B(\beta_n)}$$

Where:

$$\mathrm{A}(\beta_n) = -P_n H_{2,n}\left(1+\beta_n P_n H_{2,n}\right) - (1-\beta_n) {P_n}^2 {H_{2,n}}^2$$

$$B(\beta_n) = (1+\beta_n P_n H_{2,n})^2$$

Now compute:

$$\varphi''(\beta_n) = \frac{-\mathrm{A}(\beta_n).\, 2(1+\beta_n P_n H_{2,n}) P_n H_{2,n}}{\left(1+\beta_n P_n H_{2,n}\right)^4}$$

$$\varphi''(\beta_n) = \frac{2\mathrm{A}(\beta_n).\, P_n H_{2,n}}{\left(1+\beta_n P_n H_{2,n}\right)^3}$$

Now the final $g''(\beta_n)$ becomes:

$$g''(\beta_n) = -\frac{B_{2,n}}{\ln(2)} \cdot \left(\frac{\varphi''(1+\varphi) - (\varphi')^2}{(1+\varphi)^2} \right)$$

The full second derivative $g''(\beta_n)$ involves both the first and second derivatives of $\varphi(\beta_n)$.
$g''(\beta_n) > 0 \Rightarrow g(\beta_n)$ is convex
Thus, the DC form $f(\beta_n) - g(\beta_n)$ is valid and solvable using DC techniques.

APPENDIX B

Hessian Derivation and Concavity Analysis

To establish concavity of $f(\beta_n, P_n)$, we compute Hessian matrix:

Let

$$f\left(\beta_n, P_n\right) = B_n \cdot \log_2\left(1 + P_n\ H_{1,n}\right) + B_n \cdot \log_2\left(1 + (1-\beta_n) P_n H_{2,n}\right)$$

Where:

- P_n:power on subchannel n
- β_n: Power splitting factor.
- $H_{1,n}$, $H_{2,n}$: Channel gains of strong and weak users on subchannel n.
- B_n: subchannel bandwidth.

We compute the Hessian matrix of $f(\beta_n, P_n)$ with respect to (β_n, P_n). The Hessian is:

$$\nabla^2 f = \begin{bmatrix} \frac{d^2 f}{d\ {P_n}^2} & \frac{d^2 f}{dP_n d\beta_n} \\ \frac{d^2 f}{\mathrm{d}\beta_n\ dP_n} & \frac{d^2 f}{d\ {\beta_n}^2} \end{bmatrix}$$

- First Derivatives:

$$\frac{df}{dP_n} = \frac{B_n H_{1,n}}{\left(1 + P_n\ H_{1,n}\right) \ln 2} + \frac{B_{2,n} H_{2,n} (1 - \beta_n)}{(1 + (1 - \beta_n) P_n H_{2,n} \ln 2}$$

$$\frac{df}{d\beta_n} = \frac{-B_n P_n H_{2,n}}{(1 + (1 - \beta_n) P_n H_{2,n}) \ln 2}$$

- Second Derivatives:

$$\frac{d^2 f}{d\ {P_n}^2} = \frac{-B_n {H_{1,n}}^2}{\left(1 + P_n\ H_{1,n}\right)^2 \ln 2} - \frac{B_n {H_{2,n}}^2 (1 - \beta_n)^2}{(1 + (1 - \beta_n) P_n {H_{2,n}}^2 \ln 2}$$

Both the strong and weak user terms yield negative second derivatives, confirming concavity in P_n.

$$\frac{d^2 f}{d\ {\beta_n}^2} = \frac{-B_n\ {P_n}^2 {H_{2,n}}^2}{(1 + (1 - \beta_n) P_n H_{2,n})^2 \ln 2}$$

The expression depends only on the weak user's term and is strictly negative, confirming concavity in β_n.

- Mixed partial derivative

$$\frac{d^2 f}{dP_n d\beta_n} = \frac{d^2 f}{\mathrm{d}\beta_n\ dP_n} = \frac{-B_n H_{2,n}}{(1 + (1 - \beta_n) P_n H_{2,n})^2 \ln 2}$$

The negative value indicates that increasing β_n weakens the rate's sensitivity to P_n, aligning with NOMA power-splitting behavior. Putting all partials together, the Hessian matrix becomes:

$$\nabla^2 f(\beta_n, P_n) = \begin{bmatrix} \frac{d^2 f}{d\ {P_n}^2} & \frac{d^2 f}{dP_n d\beta_n} \\ \frac{d^2 f}{\mathrm{d}\beta_n\ dP_n} & \frac{d^2 f}{d\ {\beta_n}^2} \end{bmatrix}$$

$$= \begin{bmatrix} -\frac{B_n {H_{1,n}}^2}{\left(1 + P_n\ H_{1,n}\right)^2 \ln 2} - \frac{B_n {H_{2,n}}^2 (1 - \beta_n)^2}{(1 + (1 - \beta_n) P_n {H_{2,n}}^2 \ln 2} & -\frac{B_n H_{2,n}}{(1 + (1 - \beta_n) P_n H_{2,n})^2 \ln 2} \\ -\frac{B_n H_{2,n}}{(1 + (1 - \beta_n) P_n H_{2,n})^2 \ln 2} & -\frac{B_n\ {P_n}^2 {H_{2,n}}^2}{(1 + (1 - \beta_n) P_n H_{2,n})^2 \ln 2} \end{bmatrix}$$

Since all entries of the Hessian matrix are negative, $f(\beta_n, P_n)$ is concave in both variables. This confirms the validity of using its negative in a DC decomposition, where $-f(\beta_n, P_n)$ serves as a convex term in the optimization process.

Supplementary Files

This is a list of supplementary files associated with this preprint. Click to download.

- simresults.rar